

1 **Supplementary Materials for**

2 **Watershed-Based Evaluation of Automatic Sensor Data: Water Quality and** 3 **Hydroclimatic relationships**

4 **Jacopo Cantoni, Zahra Kalantari and Georgia Destouni**

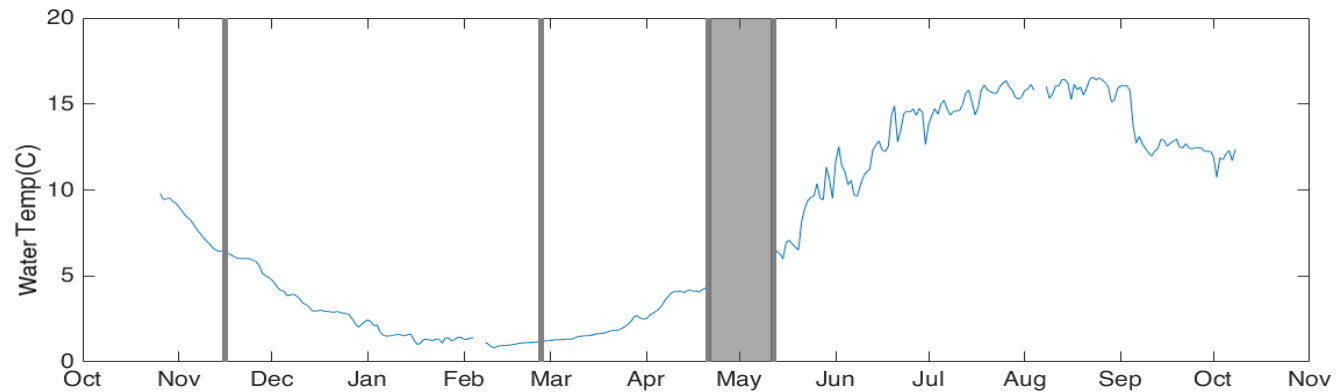
5 This supplemental material provides a description of the automatic sensor and the methodology used for water quality data collection, and a set of additional
6 graphs and figures about the water quality data from the automatic sensor and other related data: Figure S1–S12, time series of sensor-measured water quality
7 variables; Figure S13, Time series of independently measured catchment-average precipitation (P); Figure S14–S15, Time series of independently measured nutrient
8 concentrations; Figure S16, Slope and intercept values of linear regression lines between water discharge Q and water quality variables; Figure S17, Slope and
9 intercept values of linear regression lines water quality variables; Figure S18, Slope and intercept values of linear regression lines between water discharge Q and
10 nutrient concentrations.

11 **1. Automatic Sensor and Method Description**

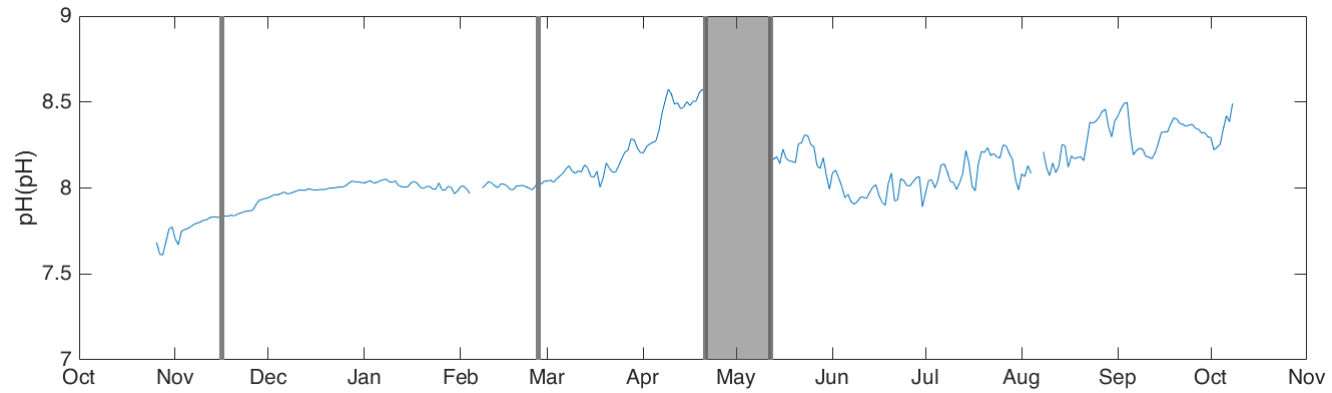
12 The water quality data were provided to us for this study as collected by the Stockholm City municipal water, wastewater, and waste handling utility “Stockholm
13 Vatten och Avfall” and their subcontractor Luode Consulting, during the period 26 October 2016–12 October 2017. The data were obtained using a YSI EXO2
14 multiparameter probe (<https://www.ysi.com/EXO2>), in combination with an automatic vertical profiler (<https://www.ysi.com/Pontoon-Vertical-Profiling-System>).
15 Specific information from YSI on all the water quality measured can be found on the YSI website: <https://www.ysi.com/parameters>. The maintenance routine during
16 the monitoring period included automatic cleaning operated by a sensor wiper before every new vertical profile (i.e., around once every hour). In addition, the
17 sensor was manually cleaned once every month. Over the measurement period, three data hiatuses occurred (5–7 February, 22 April–11 May, and 5–7 October).
18 These were due to technical issues, including clogged depth sensor (which was not part of the automatic cleaning), power failure, and ice effects. The multiparameter
19 sensor was calibrated according to manufacturer instructions before deployment, and no additional data treatment was applied besides those automatically
20 operated by the sensor. The built-in software is YSI property, and little information about it is available. The general principle is that the built-in software operates
21 with the aim of removing potential unrealistic spikes by taking 5–10 measurements over a short time interval (few seconds) to determine the final reported measured
22 variable value. Additional dataset handling is applied by us to the reported measured data, in order to harmonize the water quality dataset resolution to that of
23 other datasets used in the study and, as such, obtain all data with a comparable daily time resolution. This is done by calculating the average value of all measured
24 data of each water quality variable over each day, so that each resulting average data point is representative of the entire day, and the entire measured water
25 column. The calculation of average daily values also increases the resulting data robustness, as each of the sensor-based daily data used in the study is thereby
26 backed by more than 150 measurements per day, and each of the latter, underlying direct measurement data points is, in turn, based on a series of (5–10) actual

27 samplings made by the sensor. This implies that several hundred direct measurements underlie each sensor-based daily data value used and interpreted in the
28 study, making each of the multivariable datasets robust to instrumentation and measurement uncertainty. A few anomalously low spikes are exhibited in a total of
29 11 days within the ORP data time series. Of these, 6 daily low-spike values appear directly after start of the measurement campaign (26/10/16–31/10/16, start of
30 cluster 1, down to 230 mV; Figure S3). The remaining 5 days with low ORP spikes appear within cluster 4 (12/05/17–14/05/17, start of cluster 4, down to 280 mV;
31 08/08/17–09/08/17, down to 300 mV; Figure S3). These anomalously low spikes are likely temporary effects after sensor start or restart. To handle the few days
32 exhibiting such low ORP spikes, we replaced the associated outlier data with reasonable values, constant for each set of a couple/few consecutive days with spike
33 outliers, based on the robust daily values following the low-spike days in the ORP time series (compare the time series in Figure S4 with the spikes removed in this
34 way and that in Figure S3 with the spikes included); this adjustment was done with negligible effects and implications, as a simple way to carry out required data
35 calculations. Overall, no data used in the study exhibit values out of the sensor operability range.

36 2. Visual Representation of Time Series

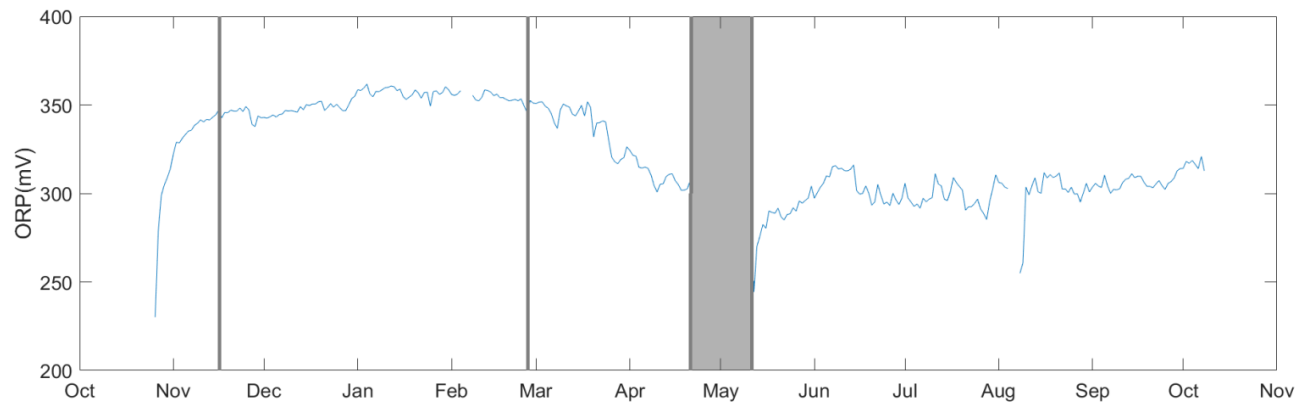


37
38 **Figure S1.** Time series of sensor-measured water temperature (T_w). The gray fields show the times of data hiatuses within the total sensor operation period October
39 2016–October 2017.



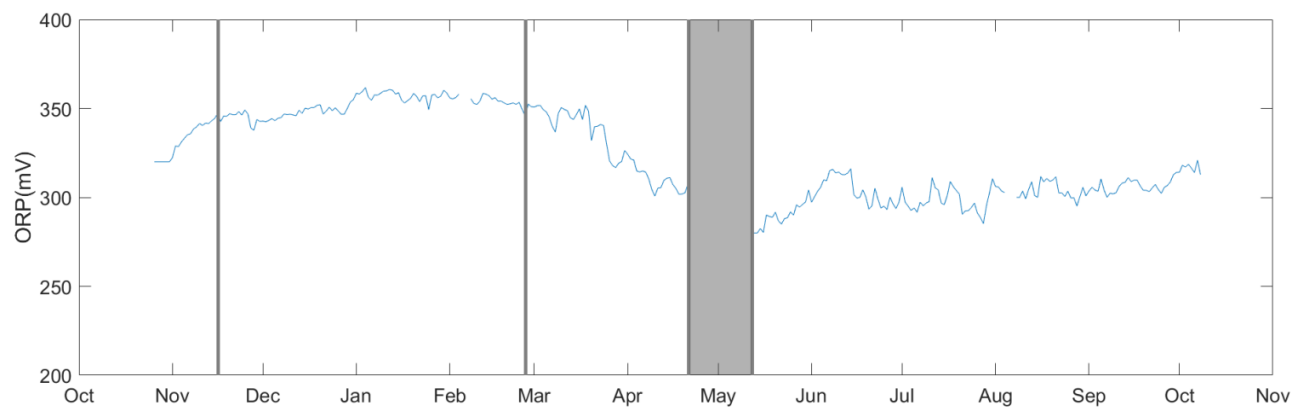
40

41 **Figure S2.** Time series of sensor-measured pH. The gray fields show the times of data hiatuses within the total sensor operation period October 2016–October 2017.



42

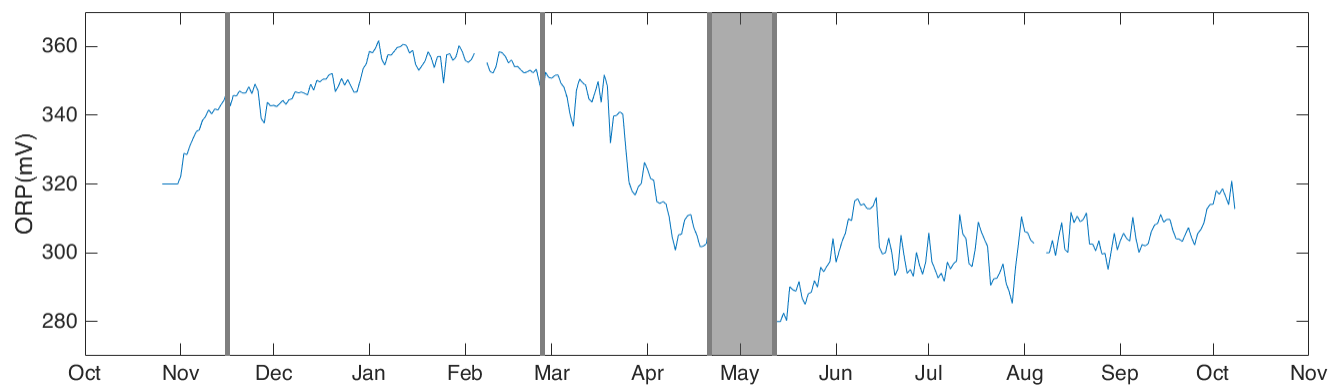
43 **Figure S3.** Time series of sensor-measured oxidation reduction potential (ORP) prior to spike removal. The gray fields show the times of sensor data hiatuses within
 44 the total study period October 2016–October 2017.



45

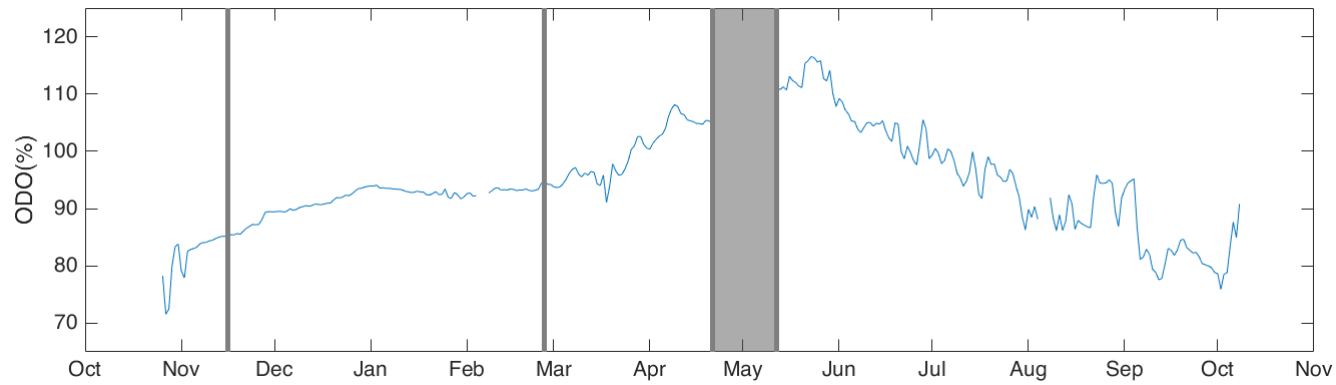
46 **Figure S4** Time series of sensor-measured oxidation reduction potential (ORP; after removal of low spike outliers). The gray fields show the times of sensor data
 47 hiatuses within the total study period October 2016–October 2017.

48



49

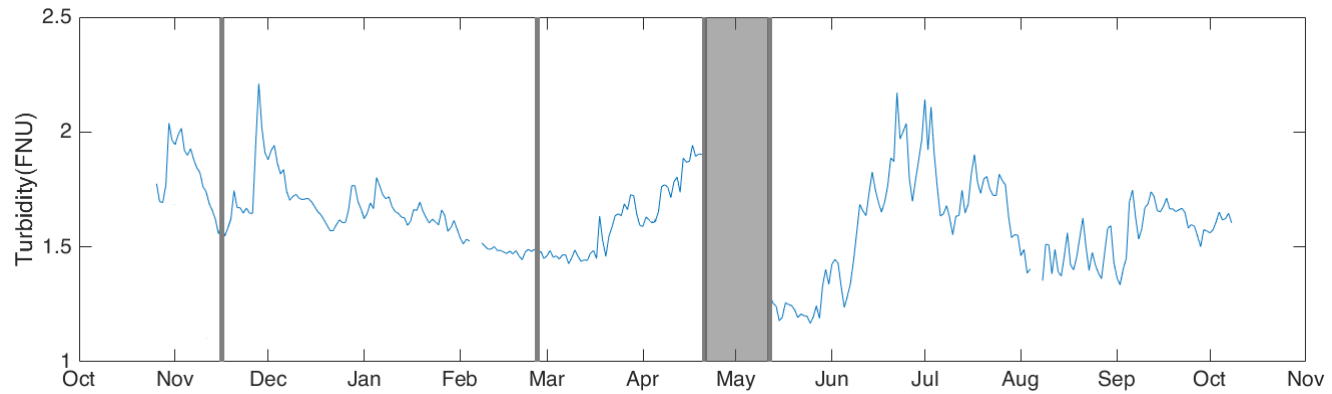
50 **Figure S5.** Time series of sensor-measured oxidation reduction potential (ORP; after removal of low spike outliers). The gray fields show the times of sensor data
 51 hiatuses within the total study period October 2016–October 2017.



52

53 **Figure S6.** Time series of sensor-measured organic dissolved oxygen (ODO). The gray fields show the times of data hiatuses within the total sensor operation period

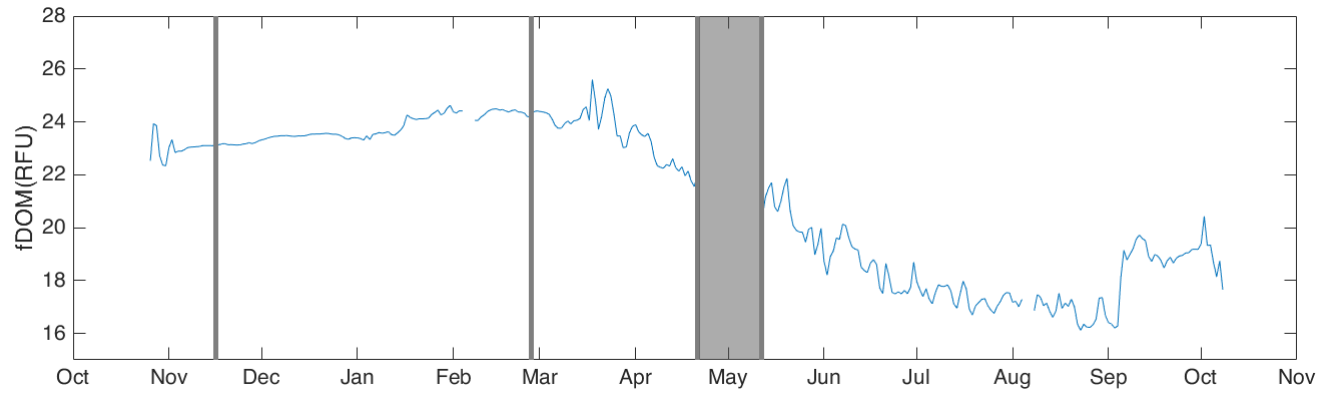
54 October 2016–October 2017.



55

56 **Figure S7.** Time series of sensor-measured turbidity. The gray fields show the times of data hiatuses within the total sensor operation period October 2016–October

57 2017.

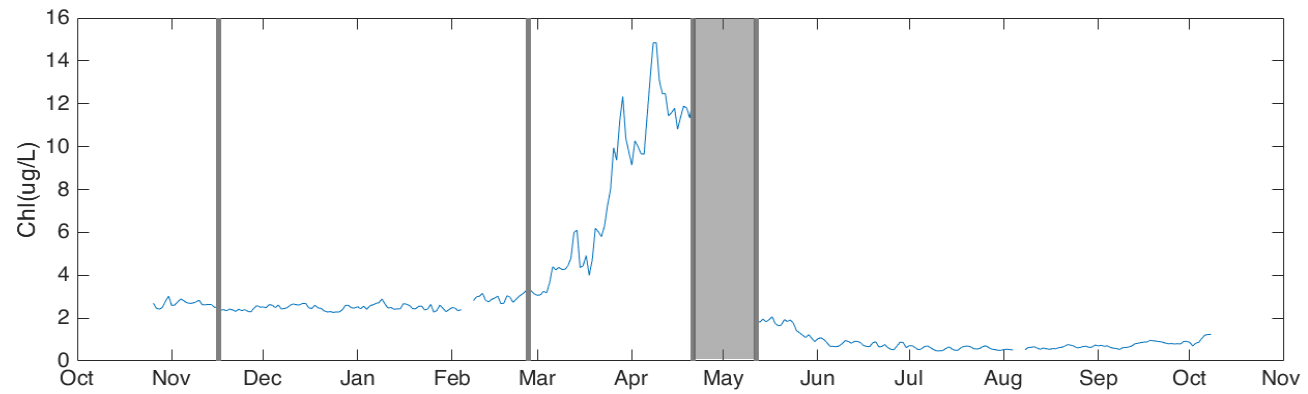


58

59 **Figure S8.** Time series of sensor-measured dissolved organic matter (fDOM). The gray fields show the times of data hiatuses within the total sensor operation period

60

October 2016–October 2017.

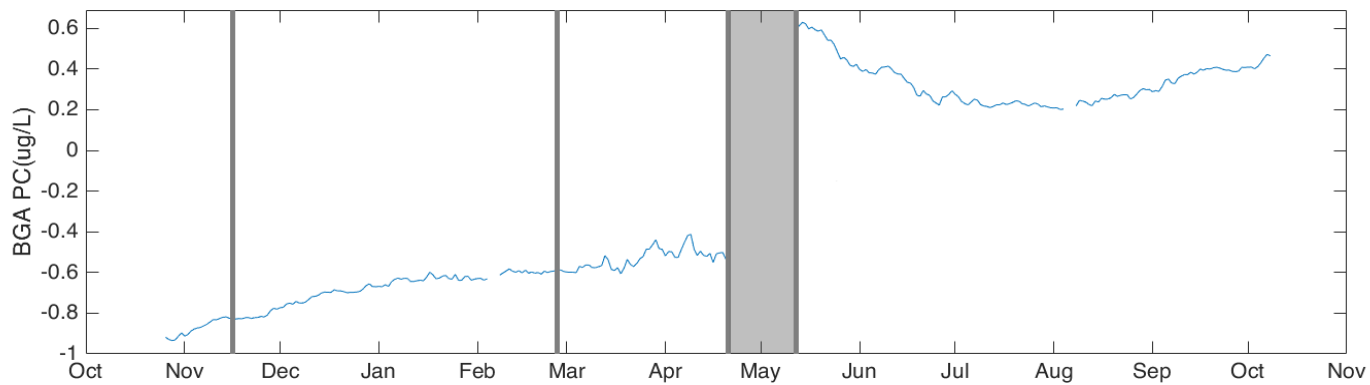


61

62 **Figure S9.** Time series of sensor-measured chlorophyll concentration (Chl). The gray fields show the times of data hiatuses within the total sensor operation period

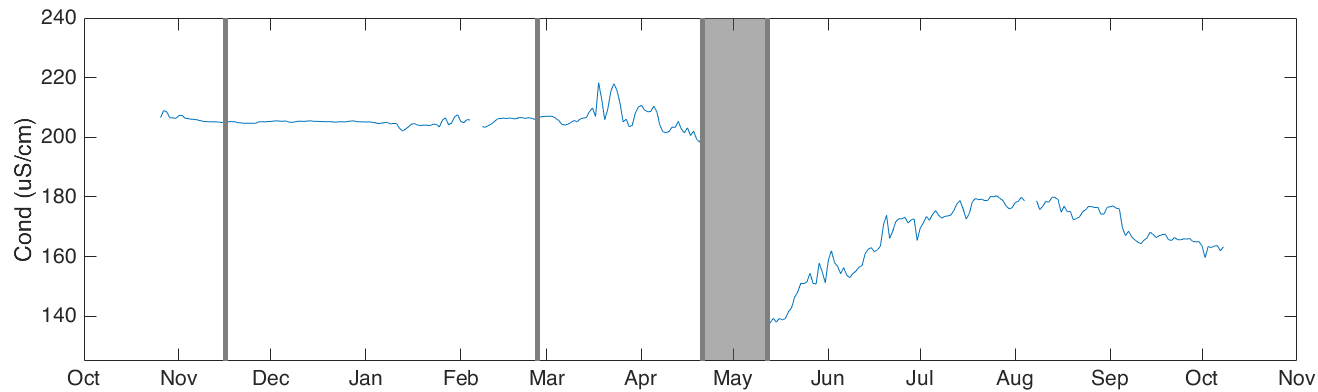
63

October 2016–October 2017.



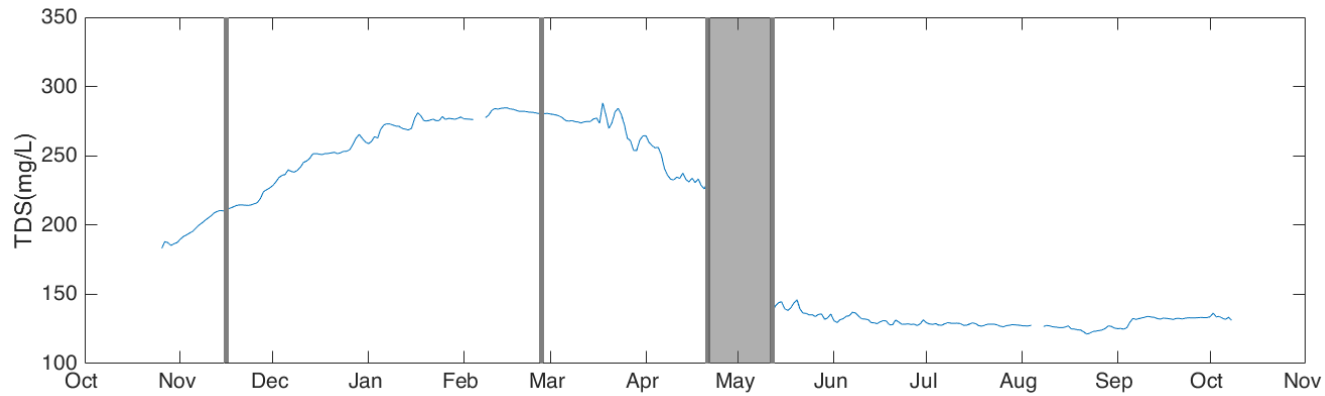
64

65 **Figure S10.** Time series of sensor-measured blue-green algae concentration (BGA). The gray fields show the times of data hiatuses within the total sensor operation
 66 period October 2016–October 2017.



67

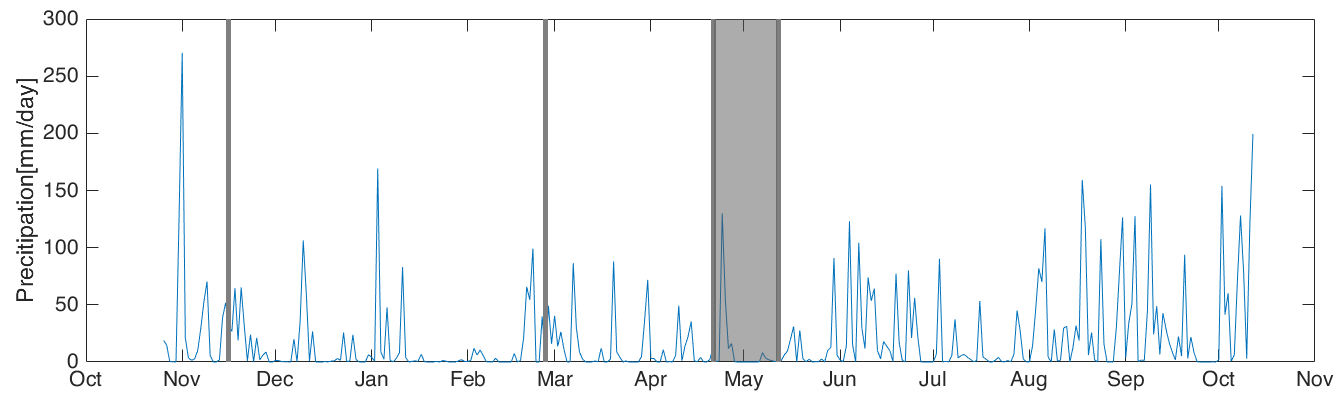
68 **Figure S11.** Time series of sensor-measured electrical conductivity (EC). The gray fields show the times of data hiatuses within the total sensor operation period
 69 October 2016–October 2017.



70

71 **Figure S12.** Time series of sensor-based estimate of total dissolved solids concentration (TDS). The gray fields show the times of data hiatuses within the total sensor
 72 operation period October 2016–October 2017.

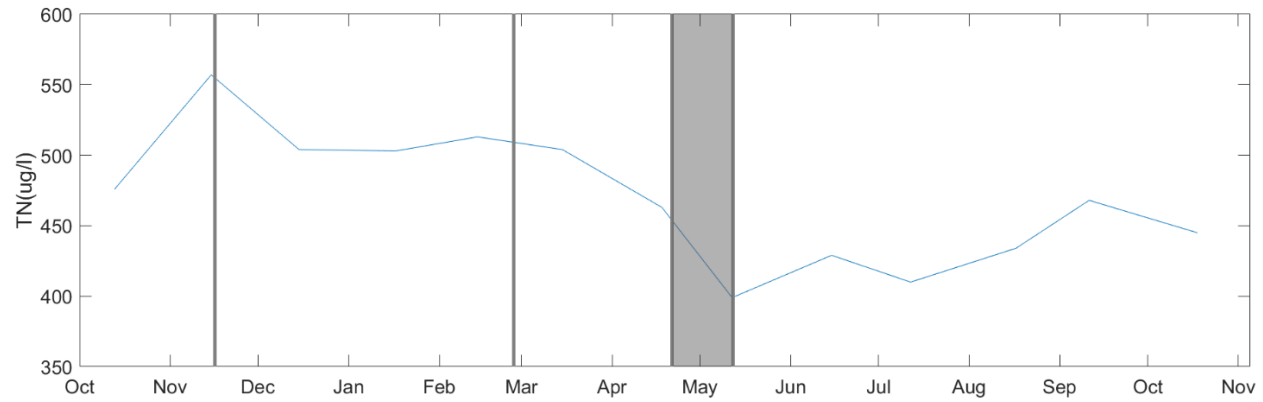
73



74

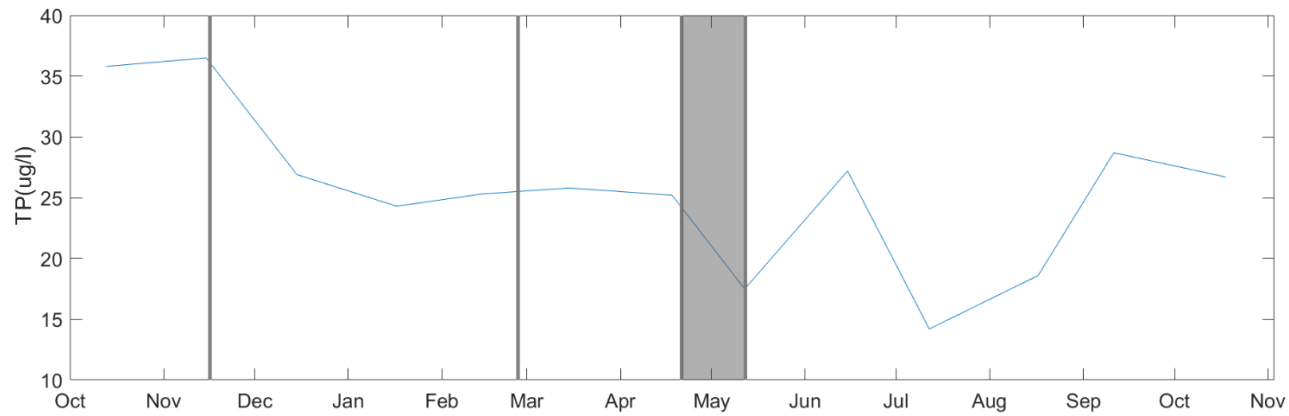
75 **Figure S13.** Time series of independently measured catchment-average precipitation (P) over the Lake Mälaren catchment. The gray fields show the times of data
 76 hiatuses within the total sensor operation period October 2016–October 2017.

77



78

79 **Figure S14.** Time series of independently measured concentration of total nitrogen (TN) at the outlet of the Lake Mälaren catchment. The gray fields show the times
 80 of data hiatuses within the total sensor operation period October 2016–October 2017.



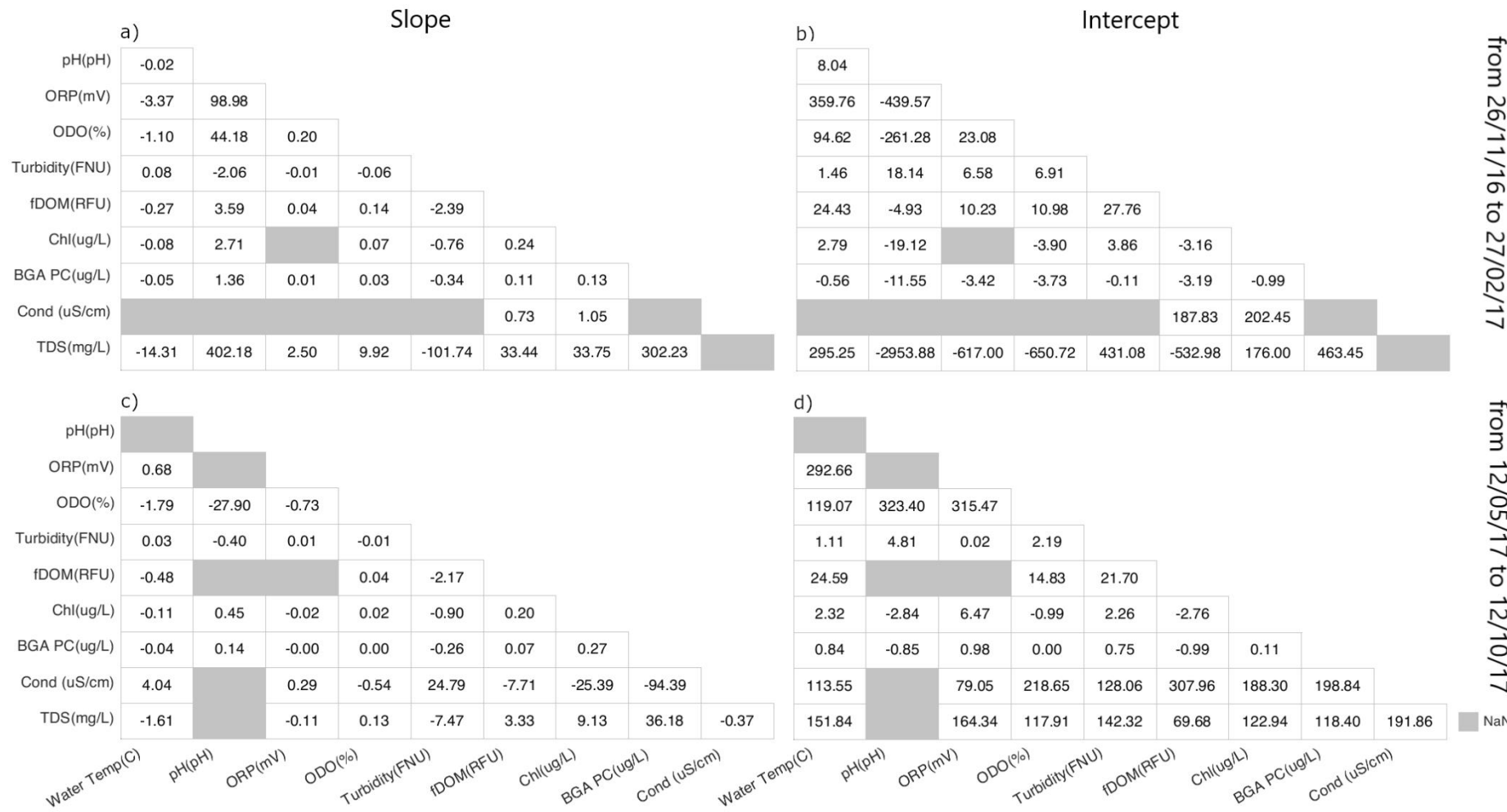
81

82 **Figure S15.** Time series of independently measured concentration of total phosphorus (TP) at the outlet of the Lake Mälaren catchment. The gray fields show the
 83 times of data hiatuses within the total sensor operation period October 2016–October 2017.

84

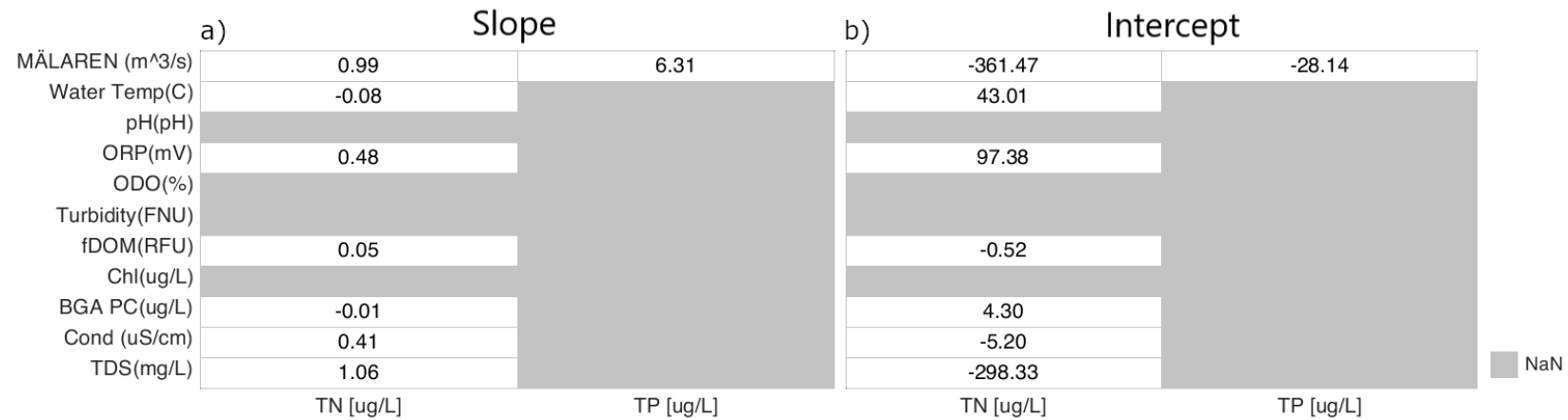
85 **3. Intercept and Slope Values of Linear Regressions**

86 This section presents the slope and intercept parameters of various linear curves obtained from linear fitting. All the variables on the vertical axes of the tables must
87 be considered y , and all the variables on the horizontal axes of the tables must be considered x . The unit of measures for intercept and slope have to be deducted
88 from the unit of the specific x and y variable under consideration. Then, the unit of measure of the intercept is the same as that of the y variable, while the slope's
89 unit is the y variable's unit divided by the x variable's unit.



94
95
96
97

Figure S17. Slope (a,c) and intercept (b,d) values of linear regression lines for different pairs of sensor-measured water quality data. Top (a,b): results for data Cluster 2 (26 November 2016–27 February 2017). Bottom (c,d): Results for data Cluster 4 (12 May–08 October 2017).



98

99

100

101

Figure S18. Slope (a) and intercept (b) values of linear regression lines for monthly data on total nitrogen (TN) or total phosphorus (TP) concentrations, and corresponding data on total discharge Q (for extended study period, 1 January 2014–26 February 2018) or sensor-measured water quality variables (for basic study period, 26 October 2016–8 October 2017), based on the days with available TN and TP data, without clustering, in each study period.